Introduction to Micro Fluidics
Patrick Tabeling
Chapter 1

ONE

Physics at the micrometric scale

1.1 Introduction

The title of this chapter, 'Physics at the micrometric scale', may seem surprising: for the physics of the systems we are discussing, it seems as if the micrometer is not inherently be a scale at which anything out of the ordinary should happen. For example, in simple liquids, molecule sizes, intermolecular distances, and correlation lengths are on the order of a *nanometer* and are thus actually much smaller than the dimensions of an ordinary microsystem. A cubic micrometer of tetradecane contains around 10^{12} atoms, a number sufficiently large to disregard the identity of the atoms, neglect thermodynamic fluctuations, and adopt without hesitation a macrometric approach. In the same way, for interfaces, the ranges of most intermolecular forces are no larger than 30 nm, a length scale that is extremely small with respect to the size of micrometric systems. In these systems, the spatial distribution of interfacial forces can be neglected without concern, and can generally be considered purely superficial, just as in macroscopic systems. Thus, one may question the necessity of dedicating an entire chapter to physics at the micrometric scale, since there does not seem to be any distinguishable differences from ordinary macroscopic physics.

However, this point of view is extreme. There are, in fact, several significant situations in microsystems where the macroscopic description must be amended, or even simply abandoned. This is indeed the case for gas flows in microcanals, whose boundary conditions include an expression for the mean free path of the gas, a quantity that is logically absent from the system of equations governing ordinary hydrodynamics. This is also the case for large molecules such as DNA or high molecular weight proteins, which must often be treated individually once they are introduced into a microsystem. Yet another example is thermal noise, which does not play an explicit role in ordinary problems of hydrodynamic

instability, but which controls the destabilization of ultraminiaturized jets. There is thus a whole collection of situations where microscopic phenomena directly intervene in the physics of systems of micrometric size, and these situations are worthy of analysis. As a final point, in many of these cases, the micrometer and nanometer are both present in the same microsystem. Furthermore, microfluidic systems equipped with nanometric detection or control elements will undoubtedly be developed in the future, thus conjugating the two scales. Extreme miniaturization will probably bring us to scales on the order of a hundred nanometers, a world intermediate between the microscopic and the nanoscopic; all these remarks justify the foray we will make in this chapter into the nanometric world.

Another question highlighted in this chapter is that of the disruption in microsystems of the equilibria of forces dominating at macroscopic scales. For example, in our 'ordinary' world, we are accustomed to the omnipresence and importance of gravitational forces. This chapter will show that at micrometric scales, gravitational forces become negligible, and the equilibria that take their place are often instead dominated by surface forces such as capillarity, wetting and adhesion. Surprising physical phenomena sometimes result, and we are forced to rationalize in a counterintuitive world. In practice, it is necessary to first determine the new equilibria that will appear in microsystems in order to know whether it will be advantageous to miniaturize. This chapter will try to accomplish precisely this goal, and will present several methods that will allow for the anticipation, without elaborate calculation, of the nature of the new equilibria dominating miniaturized systems.

In this chapter, we will first present a few elementary ideas on the sizes of different objects and the ranges of the principal intermolecular forces.

We will then analyse in the second part of this chapter the consequences of reducing the size of the system, i.e. miniaturizing, in several different situations. We accomplish this by determining the scaling laws governing the physical quantities in a given system. Nature provides us with astonishing examples of scaling laws that are not only heeded, but actually exploited by evolution.

In the third section of the chapter, we will analyse specific situations, where electrostatic, electromagnetic, mechanical, thermal, and chemical systems play a role (the hydrodynamics of microsystems is discussed in Chapter 2). The reader will note that it is often advantageous to work with miniaturized devices rather than devices operating at macrometric scales. This fact undoubtedly justifies the big expectations we have today for the field of microsystems[1].

[1] In the field of MEMS, the macrometric scale is sometimes referred to as the 'macroscopic scale'. To avoid confusion, we will not use this terminology here.

1.2 Ranges of forces of microscopic origin

1.2.1 Ranges of forces between molecules

The ranges of forces between small molecules in a vacuum do not exceed a few nanometers

We consider here the forces existing between two simple non-polar molecules, i.e. those whose barycenters of positive and negative charges overlap. Examples of non-polar molecules include the molecules of helium, nitrogen, and oxygen. When placed in a vacuum, these forces are made up of two contributions.

- The first contribution is a force of quantum-mechanical origin that can be either attractive or repulsive. In the attractive case, the force gives rise to the formation of a covalent bond. The force in the repulsive case is known as hard-sphere repulsion, and it assures the interpenetrability of atoms.
- The second contribution is from Van der Waals attraction. This term has a physical origin that can be outlined in the following manner: at a given instant, each molecule forms a dipole that deforms the electronic cloud of a neighboring molecule. When the forces generated in such a system are calculated, an attractive force is systematically produced. This polarization of a nearby molecule is known as an induced dipole-induced dipole interaction. Over the course of time, molecules and their electron clouds can fluctuate in position and in orientation, but the attractive effect always remains.

For hard-sphere repulsion, the interaction between two molecules can be described by the 'Lennard–Jones potential' $V(r)$. This potential has the following form:

$$V(r) = 4\epsilon\left(\left(\frac{\sigma}{r}\right)^{12} - \left(\frac{\sigma}{r}\right)^{6}\right), \tag{1.1}$$

where ϵ and σ are the two parameters characterizing the interaction. This potential is shown in Fig. 1.1, for helium. The parameters ϵ and σ obviously depend on which molecules are present. For example, for helium, we have the following values: $\sigma = 2.58$ Å and $\epsilon/k = 10.22$ K (here ϵ is expressed, after dividing by the Boltzmann constant k, in absolute degrees).

The force between two molecules is the opposite of the gradient of the Lennard–Jones potential. We have the following expression:

$$F(r) = -\frac{\mathrm{d}V}{\mathrm{d}r} = 24\epsilon\left(2\left(\frac{\sigma^{12}}{r^{13}}\right) - \left(\frac{\sigma^{6}}{r^{7}}\right)\right).$$

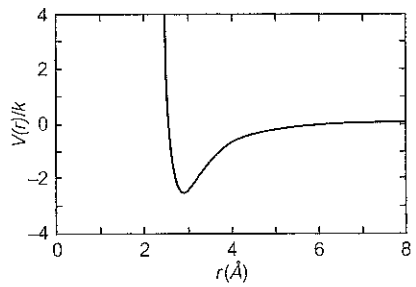

Figure 1.1 Representation of the Lennard–Jones potential for a helium molecule. The equilibrium radius, corresponding to the minimum of the potential, is 2.9 Å.

At 'large' distances, this force decreases with the inverse of the distance to the seventh power. Taking actual numerical values into account, the range of Van der Waals forces for two simple molecules can be estimated to be no more than a few nanometers. In the context of micrometric systems, these forces can thus be considered to be localized, or acting on an area of zero size, similar to an idealized point.

The above considerations apply to non-polar molecules, but once the barycenters of positive and negative charges in the molecule no longer overlap and become distinct from one another, a permanent internal dipolar moment appears and the molecule becomes polar. Water and carbon dioxide are examples of polar molecules. In these situations, there is always a hard-sphere repulsion (that has the same form as in the non-polar case) and a Van der Waals attraction. However, due to the polar character of the molecules, the attraction term includes supplementary contributions: the first is due to a permanent dipole-induced dipole interaction, and the second has a statistical origin. These terms are described thoroughly in the text of Israelachvili [1], and their presentation goes beyond the scope of this book. The important result is that these contributions decrease with $1/r^7$. We have reached the important conclusion that the Lennard–Jones potential can represent not only interactions between neutral molecules, but also those existing between isolated polar molecules in a vacuum. In the end, regardless of whether the molecule is polar, we can consider in all cases that the forces that are present do not exceed a few nanometers.

Two small molecules placed in a solvent interact in multiple ways, but over a distance of no more than a few nanometers

When two molecules are placed in a solvent—a common situation in biology and chemistry—it is obviously necessary to consider the solvent itself as a third participant in the interactions. Numerous phenomena are generated in this situation, profoundly modifying the situation described in the preceding section.

A few of these phenomena are described here, but the reader can refer to the work of Israelachvili [1] for a more complete presentation of this subject.

- When placed in a solvent such as water, an ionic crystal (e.g. salt) dissolves, and forms a collection of independent ions. The ions locally produce an electric field that tends to collect counter-ions, or the polar heads of the opposite charge, thus forming a complex and structuring the nearby environment. The charges grouped around the ion screen the electric field. Forces associated with these complexes are called hydration forces when the solvent is water.
- For certain solvents such as water, hydrogen bonds can form. A hydrogen bond is an electrostatic bond relating two electronegative ions by means of a hydrogen atom. These bonds have considerable importance in biology: dissolved in an aqueous phase, many proteins adopt a conformation determined by this type of bonding[2].

Medium-sized molecules, when placed in a solvent, interact locally with their environment

Medium-sized molecules, which have a radius of gyration (defined later) of a few nanometers, include small globular proteins and DNA fragments. Placing them in a solvent will cause the appearance of new phenomena. These phenomena are related to two factors: forces now result from the contribution of a large number of different elements, and the molecule does not have a fixed shape: it can modify its conformation as a function of its environment. This subject is vast, and only a few essentials will be given here to give a basic idea of the range of available interactions.

- When placed in an aqueous solvent, a molecule can sometimes be subjected to forces that are 'hydrophobic'. One example is a hydrophobic protein that folds on itself to minimize the contact area with the aqueous environment in which it is immersed. A 'hydrophobic' force is associated with such a conformation change, and this force is obviously not a part of the Lennard–Jones potential described previously. In the same vein, there are 'hydrophilic' forces that work to expose hydrophilic parts of the molecule to the solvent.
- Medium-sized molecules can adopt a substantial number of different conformations. We can thus legitimately introduce an entropy of conformation that the system spontaneously tries to maximize. As in all thermodynamic systems, a force can be associated with this entropy, and this force must be taken into account in the total balance of the forces present.

[2] Hydrogen bonding is also the origin of the exceptional properties of water. If there was no such thing as hydrogen bonding, water would be gaseous at ambient temperature, ice would not float on liquid water, and most of the oceans in the world would be frozen.

Despite the large variety of different situations, it seems that in all cases the ranges of forces for simple molecules involve distances that do not exceed a few nanometers. For more complex molecules of decananometric size, we can consider that the distances involved are comparable to their own size, and are thus still on a completely submicrometric scale. The case of large molecules (e.g. DNA, large proteins), whose characteristic lengths become comparable to the size of the microsystem itself, will be analysed later.

1.2.2 Ranges of intermolecular forces between surfaces

We have examined the ranges of forces acting between two molecules, be they polar or non-polar, isolated or placed in a solvent, simple or moderately complex. In this context, the ranges of forces extend no farther than a few nanometers. However, molecules can come together to form a surface and develop interaction forces with a neighboring surface. We will see that this cumulative effect results in a large augmentation of force range. It is thus important to analyse these situations, and to study at what scale in a microsystem will it become necessary to explicitly take into account the spatial structure of intermolecular forces near interfaces.

Intermolecular forces between surfaces can be measured using the surface force apparatus (SFA)

Today we have a large amount of information available on the origin and the microscopic structure of forces appearing between surfaces, in a vacuum or in the presence of liquid. The major part of the work carried out on this subject arose during the 1980s [1]. Many laboratories benefited from a remarkable device called 'the force apparatus' that allowed the approach of stages with a precision on the order of just a few angstroms [2–4], and to measure the corresponding forces with great precision. One such device is shown in Fig. 1.2.

The stage on the device is displaced in an extremely precise manner, thanks to a system of springs with varying stiffnesses, which act as a displacement divider. The space between the stages is generally measured by Fabry–Pérot interferometry [3, 4]. Information obtained using this device is presented in the form of a force–displacement curve.

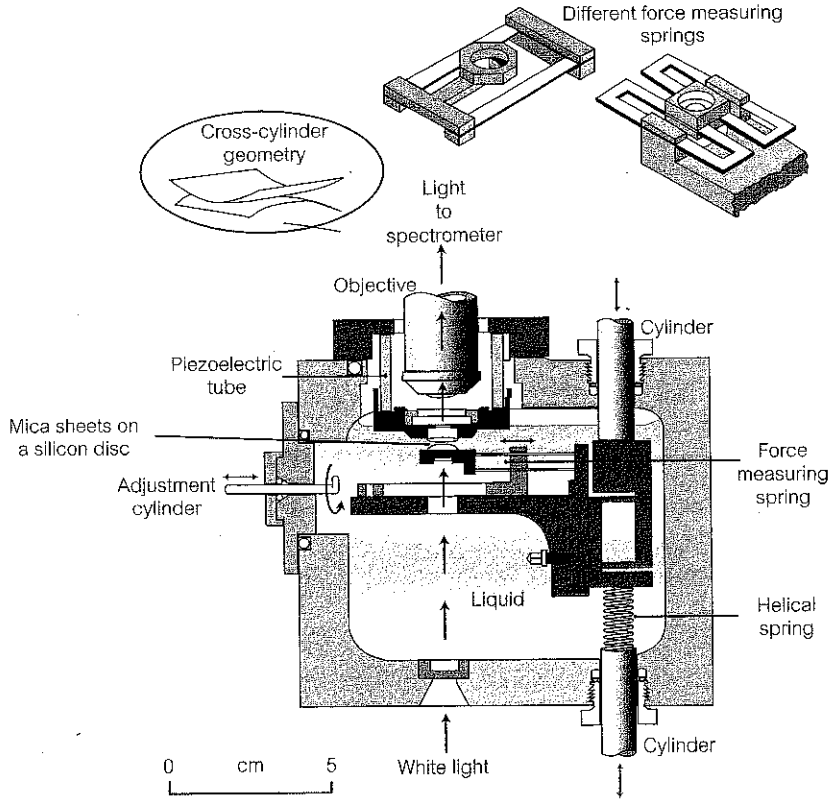

Figure 1.2 Diagram of a surface force apparatus that allowed, in the 1980s, the measurement of intermolecular forces existing near interfaces (see details in text) [1].

Classification of forces of interaction between surfaces

Of the forces of interaction between surfaces, there are those forces that act between molecules, and others that are more specifically related to the fact that we are dealing with surfaces. We conclude this section with the following list.

- **Forces of quantum origin.** These forces were introduced above in the section describing interactions between two neutral molecules. Their range is on the order of the angstrom, just as for two molecules.
- **Van der Waals forces.** We saw that the Van der Waals force varies as $1/r^7$ for molecules (where r is the distance between two molecules); this calculation shows that this same force varies as $1/r^5$ for plane–molecule systems, and as $1/r^3$ for plane–plane systems. The Van der Waals attraction force between two planes is thus written by the following formula:

$$F = -\frac{A}{6\pi r^3},$$

where A is the Hamaker constant[3]. A typical value of this constant for hydrocarbon surfaces is 5×10^{-20} J. As we will see in Chapter 3, it is generally preferable in interface problems to work in terms of energy rather than force. We thus define the energy of interaction between two planes by the quantity:

$$E = -\frac{A}{12\pi D_0^2},$$

where D_0 is the equilibrium distance between two planes, i.e. the distance where repulsive quantum forces equal the attractive Van der Waals forces. This energy is the energy of adhesion between two planes. It is written:

$$E = -\frac{A}{12\pi D_0^2} = -2\gamma,$$

where γ is the surface tension. An energy of 2γ is necessary to separate two planes bound by Van der Waals adhesion.

The spatial dependence of the intensity of Van der Waals forces was not experimentally verified in plane–plane systems, but in sphere–sphere or sphere–plane systems. For a sphere–sphere system, the calculation shows that the Van der Waals force decreases as $1/D^2$ (instead of $1/D^3$). This evolution is clearly confirmed by the experimental curve in Fig. 1.3, obtained for two surfaces of mica. This curve also shows that the range of Van der Waals forces is on the order of 10 nm.

- **Electrostatic forces.** When a dielectric is immersed in an electrolyte, a surface charge almost always spontaneously appears. For example, a plate of glass immersed in aqueous solution becomes negatively charged[4]. The origin of this phenomenon comes from the fact that the silane terminals Si–O–H localized on the glass surface lose hydrogen ions in the presence of the aqueous solution; this protonation leaves Si–O^- terminals on the surface, thus causing the

[3] It is instructive here to mention Lifschitz theory, which is applicable in the situation of two surfaces composed of non-polar molecules, separated by a vacuum [5]. This theory leads to the following formula for the Hamaker constant:

$$A = \frac{3}{4}kT\frac{\epsilon_1 - \epsilon_2}{\epsilon_1 + \epsilon_2} + \frac{3I}{16\sqrt{2}}\frac{(n_1^2 - n_2^2)^2}{(n_1^2 + n_2^2)^{3/2}},$$

an expression in which k is the Boltzmann constant, T is the absolute temperature, ϵ_1 and ϵ_2 are the dielectric constants for the environment in question, n_1 and n_2 are the optical indices, and I is their ionization potential.

[4] If the pH of the solution is greater than 4.

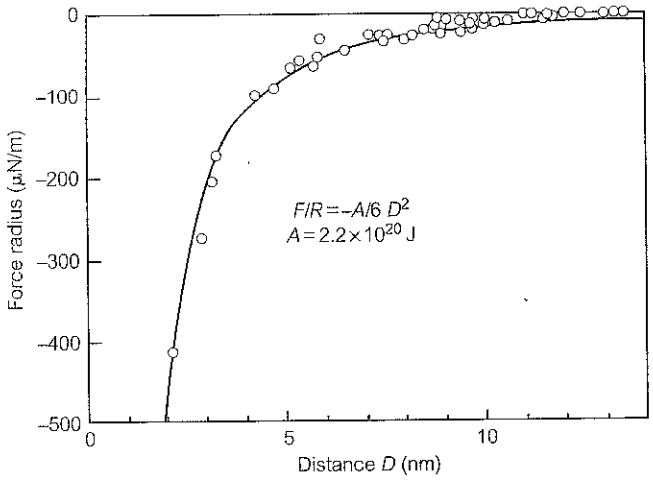

Figure 1.3 Measurement of the force between two crossed mica cylinders of radius $R \approx 1$ cm, in water. To interpret these measurements, it is necessary to note that two crossed cylinders exert attractive Van der Waals forces that are inversely proportional to the square of their distance (while forces between two planes are proportional to the cube of the distance between them). After [1].

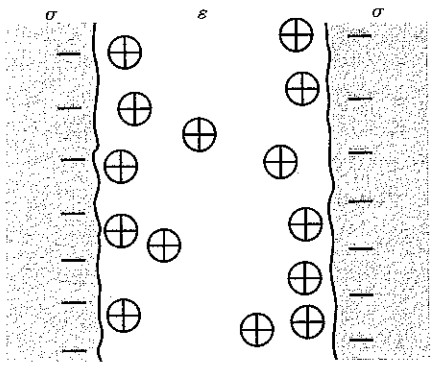

Figure 1.4 Diagram showing the formation of charged layers in the fluid and in the solid, leading to the generation of electrostatic forces. The mechanism is the following: the surfaces, when exposed to the solvent, are spontaneously charged; the counter-ions tend to migrate towards the charged surfaces, under the effect of Coulomb forces, forming a Debye–Huckel double layer.

glass exposed to aqueous solution to become negatively charged. To illustrate, the electric potential associated with these charges, for a pH of 7, is on the order of −100 mV. These processes are described in detail in the text of Cabane and Hénon [6].

These surface charges are equilibrated in the fluid by a double layer of counter-ions, as shown in Fig. 1.4.

The first layer is a molecular film of counter-ions, and is fixed at the level of the solid/liquid interface under the effect of attractive forces acting between the charged solid surfaces. This first layer is called the 'Stern layer'. It is associated with the solid by an electrostatic interaction. The second layer is not connected to the crystalline network (ordered or disordered) of the solid: it is diffuse. Its structure results from a statistical equilibrium between thermal agitation (which tends to homogenize the charge distribution) and electric forces (which tend to displace charges of the same sign towards the surface, thus creating a default in the homogeneity). The characteristics of this layer are obtained using statistical physics, worked out for the first time by Debye and Huckel. The order of magnitude of the thickness of the double layer, designated by λ (the Debye–Huckel length) is given by the following expression:

$$\lambda_D = \sqrt{\frac{D\epsilon}{\sigma}},$$

where σ is the electrical conductivity, ϵ the dielectric permittivity, and D the diffusion coefficient of the ions of the double layer. To illustrate, we can note that the double layer is a dozen nanometers thick for an ionic solution of 1 mM of salt. As λ increases proportionally with the inverse of the square root of the conductivity of the solution, it can in principle achieve high values. However, practically speaking, since it is very difficult to limit the dissolution of ions that is inevitably present on the surfaces containing the liquid, the thickness of double layers does not exceed about a hundred nanometers. This double layer is the origin of electrostatic forces, which had been measured in force machines. Figure 1.5 shows one measurement of such forces, between two mica cylinders.

The force of the double layer decreases exponentially, as the theory predicts. Figure 1.5 also indicates that the ranges of the forces of the double layer can attain several tens of nanometers.

- **Solvation forces.** When a simple liquid or a polymer melt is confined between two surfaces separated by a few nanometers, the liquid tends to structure itself, as shown in Fig. 1.6.

As the confinement increases, at some point only a few molecular layers remain between the two planes. We can imagine that the forces of interaction between the two planes will depend on this structuration effect. This type of experiment was able to show that the force is an oscillating function of the distance. The spatial period is on the order of the intermolecular distance of the liquid, and the amplitude of the associated force only decreases beyond a distance on the order of 10 nm. This force is called the solvation force.

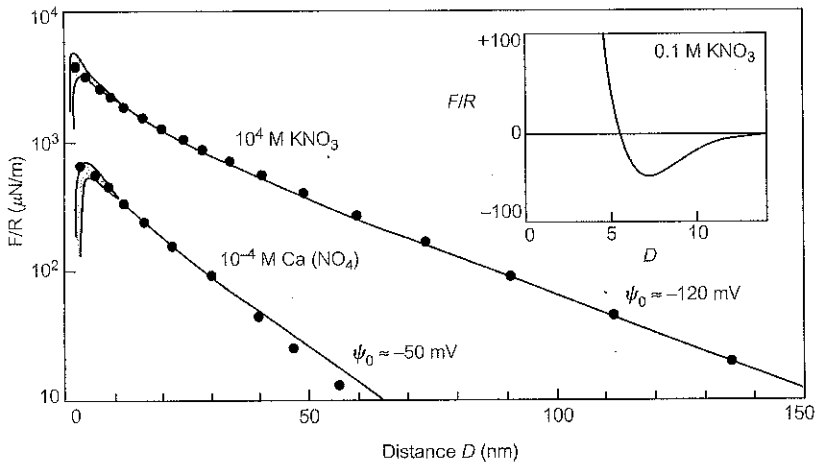

Figure 1.5 Measurement of force between two crossed mica cylinders of $R \approx 1$ cm in electrolytes. The forces of the double layer decrease exponentially with distance, and can extend over several tens of nanometers. The solutions used for this experiment are KNO_3, and $CaNO_3$ for the upper and lower curve, respectively. The continuous lines are obtained from the 'DLVO' theory, after [1].

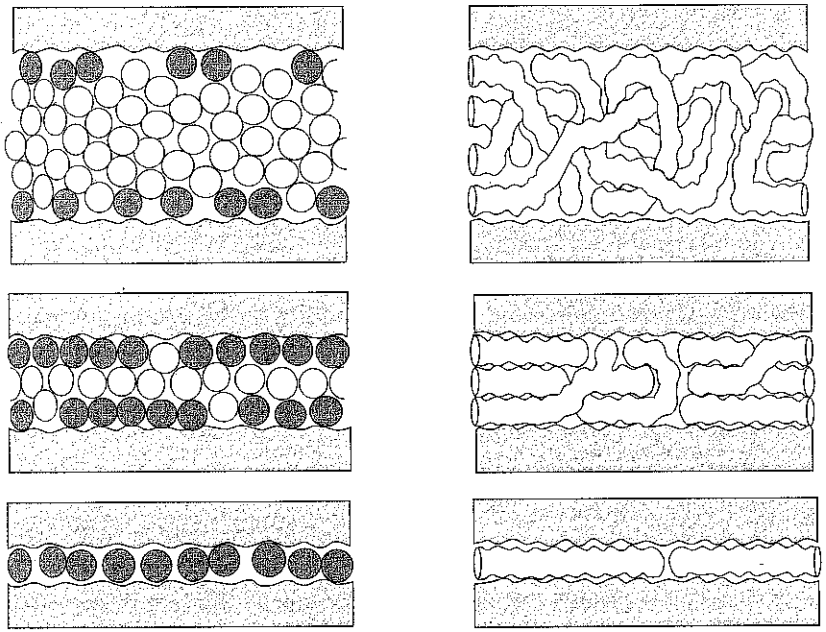

Figure 1.6 Diagram showing how a crystalline surface can affect the structure of a liquid near the liquid/solid interface, in two situations: a simple liquid (left) and a polymer melt (right). From top to bottom, the confinement increases until the system reaches a situation where one single molecular layer can insert itself between the solid surfaces.

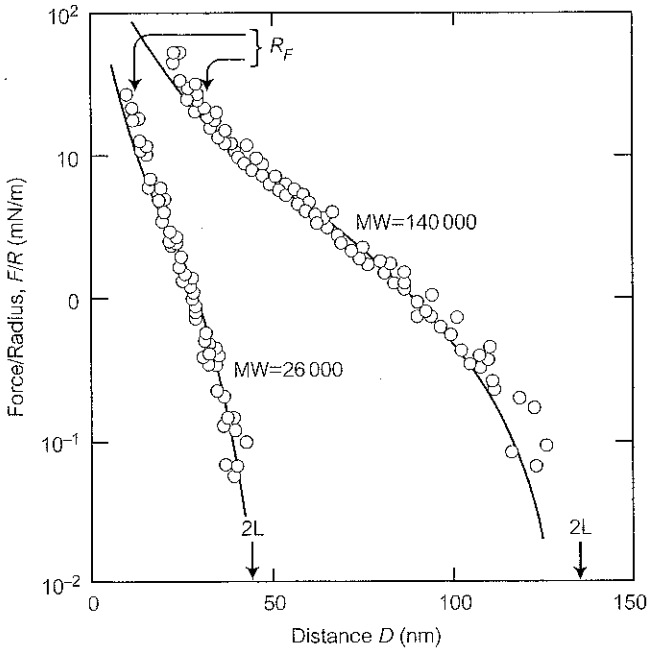

Figure 1.7 Forces between two surfaces of mica functionalized by layers of polystyrene [7]. Two situations are represented here, corresponding to two different molecular weights (MW) of polystyrene. The continuous lines represent the theory of Alexander de Gennes.

• **Forces related to fluctuations.** Other forces play a part in the specific case where surfaces are functionalized (i.e. covered by one or several molecular layers adsorbed to the surface, modifiying its physicochemical properties). The curve in Fig. 1.7 shows one case where the surface of mica is functionalized by the adsorption of polystyrene molecules. In this case, there exists a repulsion effect between the two surfaces that extends over several tens of nanometers. To understand the origin of this effect intuitively, it is necessary to consider that the molecules functionalizing the surface are not rigidly bonded to the surface; their positions fluctuate considerably, and these fluctuations make the layer seem much thicker than it actually is.

• **In conclusion,** the range of interactions between planes is much larger than interactions between two molecules. In practice, this range does not go beyond 100 nm. In terms of 'standard' microsytsems (i.e. systems a few tens of micrometers in size), intermolecular forces can be considered to be localized, i.e. applied to regions of zero thickness. These systems could be treated by methods analogous to those used in macroscopic systems. In particular, it will be

logical to introduce the idea of 'capillarity', which we will develop in Chapter 2. In ultraminiaturized systems, which have tranverse dimensions less than a hundred or so nanometers, we expect that effects directly related to the spatial extension of Van der Waals forces will appear at the extension of the double layer. We enter here into the domain of nanofluidics, which we have mentioned several times in this text. By way of example, we can refer to an experiment carried out in a nanocanal that allowed the indirect characterization of the internal structure of the double layer [8]. There still has not been experimental proof the spatial structure of Van der Waals forces in an ultraminiaturized microsystem. As we mentioned above, experimental systems have allowed the successful analysis of intermolecular forces acting between surfaces using force apparatuses, and these can be classified as 'traditional' mechanical systems.

1.3 Microscopic scales intervening in liquids and gases

Scales involved in gas and simple liquid systems are as follows:

- The sizes of molecules are usually defined by the distance at which the Lennard–Jones potential, given by the relation (1.1), is at a minimum. This value is the equilibrium radius of the pair of molecules in interaction. This quantity is (see equation (1.1)):

$$r_e = 2^{1/6}\sigma.$$

  For simple molecules, these values are on the order of a few angstroms.
- A second important scale is the average distance between molecules. A relation often used is that relating the density n and the average intermolecular distance d:

$$d = n^{1/3}.$$

  We know that for a liquid, the size of the molecule is comparable to the intermolecular distance, while for a gas, the former is much smaller than the latter.
- For gases, the fundamental scale necessary to establish dynamical properties is neither r_e nor d, but the mean free path λ. This scale is defined as the average distance travelled by a molecule between two successive collisions. The kinetic theory of gases allows the following expression to be established:

$$\lambda = \frac{1}{\sqrt{2}\pi n a^2} = \frac{kT}{\sqrt{2}\pi p a^2},$$

  where n is the density (the number of molecules per unit volume), T is the temperature, k is the Boltzmann constant, p is the pressure, and a the size of the molecule.

What is the order of magnitude of a mean free path for air?

We can estimate this value from the preceding formulas: Avogadro's law stipulates that all gases contain the same number of molecules per unit volume; at ordinary pressure, and at a temperature of 273 K, this number is 2.69×10^{19} cm^{-3}. For air, assuming that the size of the molecule is on the order of 3 Å, we obtain a mean free path of around 60 nm. However, in practice the determination of the mean free path is made from viscosity measurements given by the kinetic theory of gases.

We thus obtain a list of values of the mean free path for different gases [9][5], shown in the table below.

Gas	λ (nm)
Air	61
Nitrogen	60
Argon	64
Helium	177

It seems that under normal conditions, the mean free path is a (small) fraction of a micrometer. It is obvious that this scale must be explicitly considered once the dimensions of the microcanals are on the order of magnitude of a micrometer. We will analyse the hydrodynamic consequences of this in the following chapter.

[5] For reasons that are not well understood, the values of the mean free path of gases vary from one publication to another by about 10%. The values shown in the table have been taken from [9]. They are consistent with known values of gas viscosities.

1.4 Micromanipulation of molecules and cells in microsystems

1.4.1 Introduction

Microsystems allow for the micromanipulation of macromolecules, such as DNA, individually. The first experiment involving controlled stretching of a molecule of individual DNA was carried out at the intersection of two microcanals etched in silicon [10]. After the success of this experiment, other experimental setups based on more traditional techniques allowed the study of the elasticity of DNA with excellent precision, and the analysis of phenomena such as the coiling of the molecule under a variety of conditions [12].

Microsystems also permit the micromanipulation of biological cells. At this time, many experiments have shown that it is possible to trap, carry out transfection, electroporate, and lyse cells individually, and in a controlled manner in microsystems [13–15]. This type of manipulation is not new in the domain of biophysics. However, the fact remains that microsystems allow integration and parallelism, which open up promising possibilites in fields like biology.

In this section, we give some general information on the size of objects contributing to distinctive experimental studies carried out in microsystems, and we will then mention a few specific studies performed on the subject.

1.4.2 Generalizations on the sizes of macromolecules

Macromolecules are molecules containing a large number (between a few thousand and millions) of atoms: they include proteins, DNA, and polymers. Figure 1.8 represents three molecules of biological interest, developing the idea of the differences in size between ordinary molecules and large macromolecules.

Depending on their crystallographic structure, the solvent in which they are immersed, or the temperature, macromolecules can adopt different shapes: helices, globules, sheets, stretched structures, etc.[6].

[6] The form of macromolecules is characterized by their structure. Generally, four levels of structure are distinguishable: primary, secondary, tertiary, and quaternary. The primary structure of a protein is the sequence of amino acid residues making up the polypeptide chain. The secondary structure characterizes the spatial arrangement of the base units of the chain (for example, in the form of a helix or a sheet). The tertiary structure corresponds to the overall form of the macromolecule (globular, stretched-out, etc.) and the quaternary structure comes into play when the macromolecule itself forms several types of molecular assemblies.

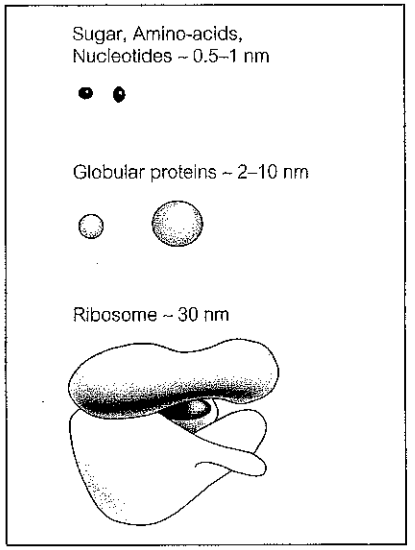

Figure 1.8 Figure showing three molecules of different sizes: the largest molecules here are enzymes, which typically have sizes (more precisely, radii of gyration, in a non-denatured conformation) on the order of a few tens of nanometers. The smallest are simple molecules, whose sizes are on the order of a few angstroms. The small globular proteins have a size of a few nanometers.

Figure 1.9 Fluorescent signature of a partially extended 16-lambda DNA. The contour length is 336 μm. (Courtesy of Professor Steve Chu, Physics Department, Stanford University.)

Figures 1.9 and 1.10 show two macromolecules, one stretched out, and the other in a folded form.

Three geometric measurements are important to know:

- The contour length R_c is the length of the macromolecule measured along its backbone. For a polymer made up of N monomers, each separated by a distance l, we have:

$$R_c = Nl.$$

- the radius of gyration R_g, which for a macromolecule shaped around a frame represents the average distance between the extremities of that frame, while the molecule is in a folded form. We have the following relation, obtained by comparing the position of each atom along the frame to a Brownian step:

$$R_g \sim N^{1/2},$$

where N is the number of atoms making up the molecule;

- the persistence length, which characterizes the correlation length measured along the frame of the molecule.

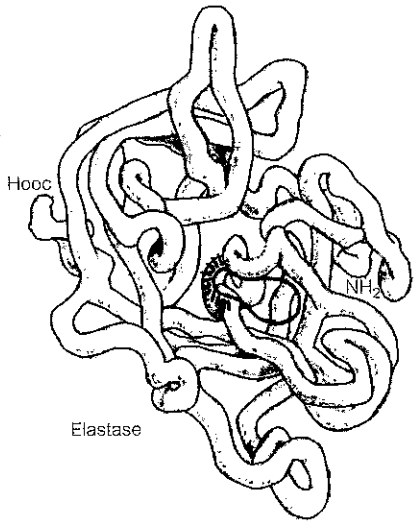

Figure 1.10 Representation of the protein elastase.

The table below gives a few orders of magnitude for DNA.

Molecule	Contour length	Radius of gyration
DNA of a human chromosome	5 cm	1 μm
DNA of the bacteria *E. Coli*	1.5 mm	100 nm

We see that the scales associated with DNA are not far from the sizes of micrometric systems. It is thus possible, in principle, to individually micromanipulate these molecules in microsystems. In such a context, we leave macroscopic hypotheses behind. The physics involved in these systems is often referred to as 'the physics of the single object'.

1.4.3 Sizes of some objects significant in biology

Macromolecules can assemble themselves to form molecular structures, and nature has obviously produced an immeasurable variety of them. Considering the large extent of this subject, only the animal cell will be described here, because the animal cell includes several molecular structures. The dimensions of these complex assemblies seem to satisfy the conditions for individual micromanipulation in the framework of microsystems. The size of an animal cell is between 10 and 30 μm. A diagram of the principal cellular elements is shown in Fig. 1.11.

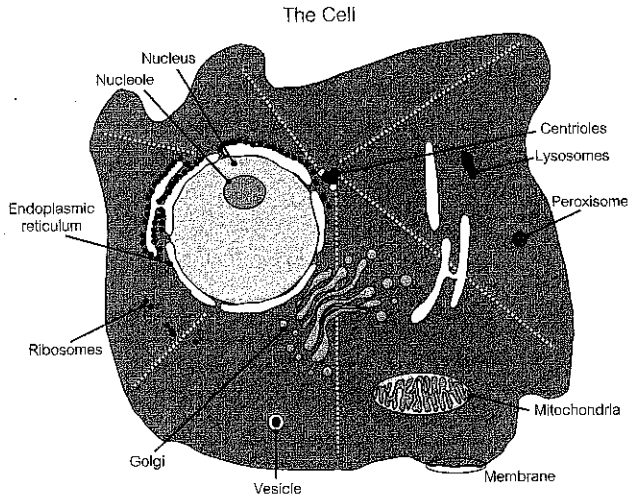

Figure 1.11 Diagram of a cell, with its major structures.

The cell is made up of several different elements:

- a nucleus of size between 3 and 10 μm. The nucleus itself is a complex object that contains, among other elements, DNA folded into the form of a chromosome. Chromosomes are objects of micrometric size;
- mitochondria, which are nucleated cells of micrometric size. Mitochondria have the cellular function of supplying energy to the cell[7];
- the endoplasmic reticulum, a collection of vesicles across which proteins are fabricated and transported. The vesicles of the reticulum are micrometric objects;
- the cytoskeleton, containing actin, tubulin, and intermediate filaments. These objects are between 10 and 30 nm in diameter, and a few micrometer in length. They ensure the mechanical cohesion of the cell;
- the cellular membrane, which has a thickness of a few tens of nanometers.

The table below presents the size of different types of cells, cellular elements, or different objects of biological significance.

[7] Mitochondria are reservoirs of ADP (acid diphosphate); the transformation of ADP to ATP (acid triphosphate), outside the mitonchondria, supplies the cell with energy.

Element	Size
Amino acid	0.8 nm
Diameter of a DNA helix	2 nm
Globular protein	4 nm
Thickness of a cellular membrane	10 nm
Diameter of a microtubule	25 nm
Large virus	100 nm
Lysosome	200 nm
Prokaryote	1–10 μm
Bacteria *E. Coli*	2 μm
Mitochondria	3 μm
Eukaryote	10–30 μm
Amoeba	90 μm
Frog oocyte	2 mm

We thus see that, in principle, the sizes of these objects lend themselves well to experimental study in microsystems. The following section will discuss a few of these experiments on DNA and the cell, which were studied individually.

1.4.4 Experiments on the micromanipulation of DNA and cells in microsystems

There exist several physical experiments carried out on DNA or biological cells using microsystems. In the vast majority of cases, these experiments are devised to offer an alternative to biological protocols, which most often treat large populations of objects (eventually polydisperse), and not isolated objects.

However, the experiment of Chu [16] is an important exception. Chu was the first to study an individual strand of DNA in a microsystem. The motivation for the experiment was a physical study of the dynamics of the molecule. In such an experiment, one end of the molecule is fixed onto a bead, and the bead is placed at the intersection of microcanals made by etching in silicon (Fig. 1.12)(these fabrication techniques will be described in Chapter 6). Figure 1.13 represents a series of photographs showing the evolution of the fluorescent signature of the DNA of a flexible bacteriophage λ. This DNA has a contour length of 22 μm, and is put under the influence of shear[8]. This type of image shows the considerable richness of the conformational dynamics of a long molecule placed in a fluid flow[9].

[8] The setup is different from that of Fig. 1.12.

[9] Among other things, these observations are useful for the problem of the reduction of hydrodynamic drag in the presence of polymers.

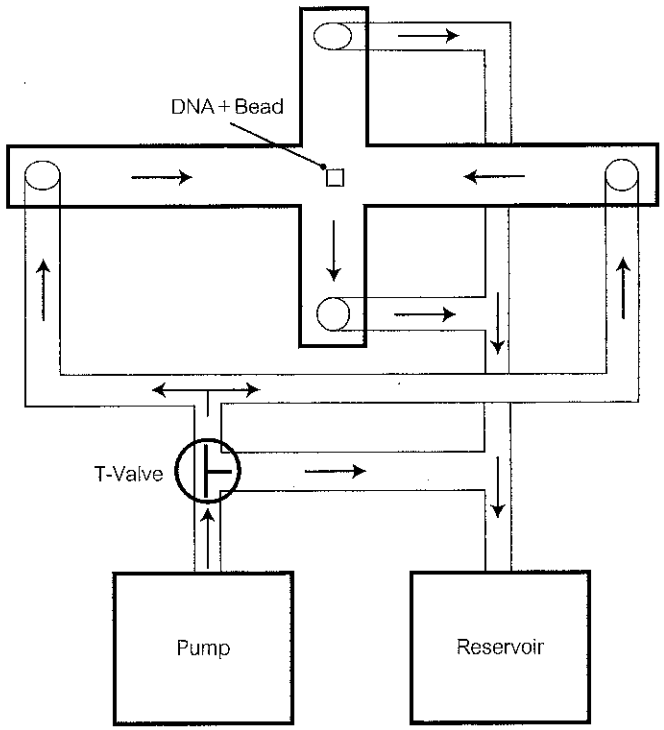

Figure 1.12 Experimental setup allowing for the study of dynamic stretching phenomena on an individual DNA molecule.

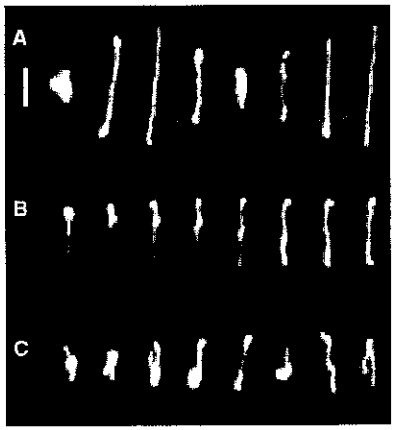

Figure 1.13 Different conformations of a DNA molecule placed in a field of pure shear, characterized by a rate of shear of 1 s^{-1}, in a viscous solution of sucrose (photo published with the permission of D.E. Smith et al., *Sciences*, 283, 1999. (Copyright 2003. American Association for the Advancement of Science).

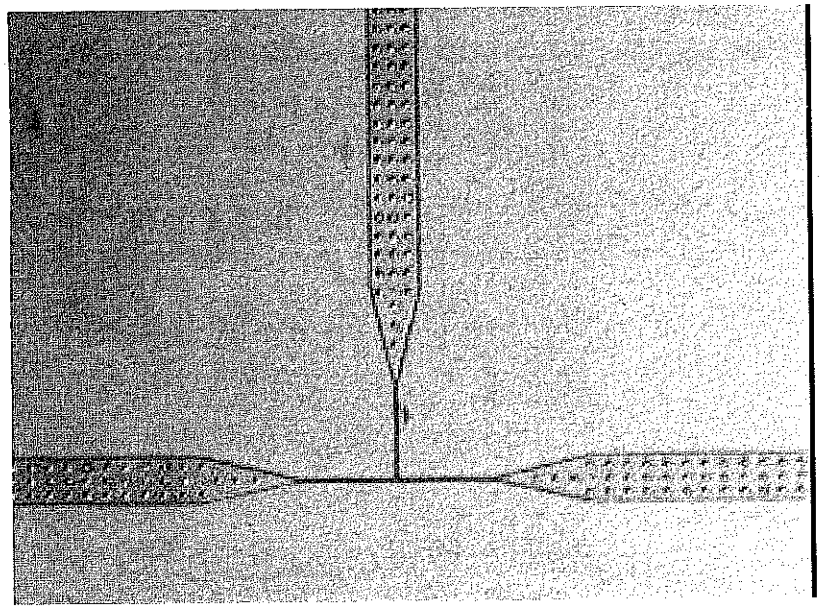

Figure 1.14 Microcytometer sorting cells one by one. Canals have a height of 3 μm; far from the intersection, they are 100 μm wide; at the intersection, their width is reduced to 5 μm; these canals were made of PDMS (see Chapter 6). The circles appearing in the microcanals are pillars preventing the collapse of the PDMS. This system is also used for sorting DNA molecules [22].

As for the micromanipulation of biological cells, there are several experimental setups that allow several elementary operations to be carried out, including lysis, transfection, characterization, etc. [14, 17, 18].

Figure 1.14 shows an example of microcytometry, which allows the measurement and sorting of cells, one by one. The proof of principle experiment was performed on *E. Coli* cells labelled with fluorescent genes (GDP)[10]; this system was later integrated [19]. Other microcytometers acting on the individual cell itself have been created [15, 20].

Systems of cellular micromanipulation will likely continue to develop in the future. Being capable of acting at the cellular level effectively provides original solutions to problems that were difficult to solve by traditional methods. Other motivations based on biological considerations emphasize the interest in acting at the level of the individual cell: in the field of neurology, the fact that the proteome[11] differs from one cell to another, and that the cells cannot be cultured, necessitates the use of the single-cell approach.

[10] In a slightly different system from that shown in Fig. 1.14.
[11] The proteome is a collection of proteins of a given system.

1.5 The physics of miniaturization

1.5.1 Introduction

In the preceding pages, we analysed scales involved in several micro/mesoscopic phenomena. Here, physical phenomena are no longer considered alone, but in relation with others. The objective of this section is to determine where equilibrium points are situated (mechanical or otherwise) in micrometric systems, and how the equilibrium is transformed when decimetric-sized systems (designated as 'macrometric' or 'ordinary' systems) are miniaturized.

1.5.2 Scaling laws for a few physical quantities

To analyse the equilibria prevailing in miniaturized systems, it is useful to introduce the idea of the scaling law . A 'scaling law' signifies: the law of the variation of physical quantities with the size l of the system or the object in question. Table 1.1 presents such laws for a few physical quantities. Here, the scale l can be understood in two ways:

- the object is isotropic (having the same dimensions, by order of magnitude, in the three spatial dimensions). Here, the scale simply represents the order of magnitude of the size of the object;
- the object is anisotropic. For example, a microcanal is anisotropic as its length is generally larger that its width and height. In this case, the quantity l must be understood to be a scale controling all dimensions of the system; when l decreases (length, height, etc.), all the dimensions of the system also decrease while maintaining constant aspect ratios.

We comment here on Table 1.1. It is clear that for certain quantities, the scaling law is obvious. This is the case for mass and volume, where we have the law:

$$M \sim V \sim l^3,$$

where M is the mass and V the volume of an object of size l. An analogous commentary can be made on distance and time. However, in the majority of cases, the relation between the quantity under consideration and the scale of the system implicates other physical quantities. There are two possibilities:

- the physical quantities that intervene in the scaling law are constants. This is the case for Van der Waals forces (per unit surface) between two planar interfaces,

Table 1.1 Scaling laws for different physical quantities

Quantity	Scaling law
Intermolecular Van der Waals force	l^{-7}
Density of Van der Waals force between interfaces	l^{-3}
Time	l^0
Capillary force	l^1
Distance	l^1
Flow velocity	l^1
Thermal power transferred by conduction	l^1
Electrostatic force	l^2
Diffusion time	l^2
Volume	l^3
Mass	l^3
Force of gravity	l^3
Magnetic force with an exterior field	l^3
Magnetic force without an exterior field	l^4
Electrical motive power	l^3
Centrifugal force	l^4

whose expression is:

$$F_V = -\frac{A}{6\pi l^3},$$

where A is the Hamaker constant, already introduced in this chapter. We also obtain for the density of Van der Waals force the obvious relation:

$$F_V \sim l^{-3},$$

as Table 1.1 indicates;

– physical quantities appearing in the scaling law eventually depend on the scale. This is the case for electrostatic forces, where besides the size of the system, the electric field and the dielectric constant of the surroundings intervene. We have the following expression for the electrostatic force F_e:

$$F_e \sim \epsilon E^2 l^2,$$

where ϵ is the dielectric constant of the environment in question and E is the electric field in the system[12]. To reach the expression shown in Table 1.1, the electric field must be assumed to be fixed. In this case, one tries to estimate the maximum forces that miniaturized electrostatic systems can develop.

[12] We will justify the expression used here later.

These forces are also assumed to function near the electric field break-off point, which is treated as a constant. A similar hypothesis is made for electromagnetic forces, where the current density producing the magnetic field is considered fixed.

We comment on the exponent of the flow velocity, which is equal to 1: we assume here that the pressure difference causing fluid motion in a canal is fixed. Everywhere else, we place ourselves in a 'microfluidic' context, where the flow regime is laminar. Applying Stokes' law, we obtain in terms of order of magnitude:

$$U \sim \frac{b^2 \Delta P}{\mu L},$$

where μ is the fluid viscosity, ΔP is the pressure difference applied along the canal, L the canal length, and b its transverse dimension. From the standpoint of scaling laws, we thus have at fixed pressure difference: $U \sim l$. Thus, we arrive at the conclusion that in a typical microfluidic flow situation (a fluid circulating through a microcanal at a fixed pressure difference), the exponent associated with the velocity is equal to one. This does not imply that the exponent associated with the velocity of an object is equal to one in all cases. Such an assumption would indeed be incorrect: one counterexample can be found in the maximum velocities of animals, which are largely independent of their size.

After making these considerations, the general rule of thumb is the following: when two forces are present, it is the force associated with the weaker exponent that becomes dominant in miniaturized systems. Thus, we begin to understand that the equilibria we are used to in the macrometric world can be disrupted at the micrometric scale. For example, when the exponent of the forces of gravity is compared to that of capillary forces, one can conclude, or very nearly so (we will return to this in section 5.5) that the forces of gravity are negligible with respect to capillary forces. This situation is the inverse of the situation in the macrometric world. We will later present a few illustrations of this concept using examples drawn from nature.

1.5.3 The Π theorem

It is useful to review here the theorem of the product, called the 'Π theorem', which allows the reduction of the effective number of variables of a system, and the prediction of the consequences of miniaturization. We will not give a demonstration of this theorem; the reader can find this in most works of fluid

mechanics (see, for example, reference [23]). A classical presentation involves the definition of matrices and the determination of their row by calculating the number of variables without independent dimension. We present the result in a more compact but equivalent form:

$$A = f(a_1, a_2, \ldots, a_n)$$

in a system of units consisting of k independent units, this law can be shown to be written:

$$\Pi = g(\pi_1, \pi_2, \ldots \pi_{n-k}),$$

where the πs are the dimensionless products formed from the initial quantities. We now only have a relation between $n - k + 1$ (instead of $n + 1$) variables, which can often represent a considerable simplification with respect to the initial law. This theorem has numerous applications, notably in fluid mechanics and thermal physics. It allows the determination of the effect of scaling changes by the analysis of the evolution of dimensionless numbers governing the problem. We study an example of the simple utilization of this theorem in the context of microsystems. How do fluid flows behave in miniaturized systems, for incompressible Newtonian fluids? If the Π theorem is used to respond to this question, the local velocity u (assumed to be stationary) must be written as functions of the following parameters:

$$\boldsymbol{u} = f(\boldsymbol{x}, l, \Delta P, \mu, \rho),$$

where $\boldsymbol{x}$ is the spatial coordinate, l is the characteristic scale of the system, ΔP is the pressure difference causing the flow, μ is the viscosity and ρ is the volumetric mass of the fluid. We also here have $k = 3$ amd $n = 5$. We deduce that we can form $n+1-k = 3$ independent dimensionless numbers, which we have chosen to equal:

$$\frac{\boldsymbol{x}}{l}, \quad \frac{\boldsymbol{u}}{U} \quad \text{and} \quad \frac{Ul}{\nu},$$

where U is a velocity equal to $\Delta Pl/\mu$, and $\nu = \mu/\rho$ is the kinematic viscosity. The product Ul/ν is known as the Reynolds number Re. Thus, the preceding relation can be written in the form: $\boldsymbol{u}/U = f(Re, \boldsymbol{x}/l)$. We thus have a much simpler expression than the initial expression. In Chapter 2, we will demonstrate numerous consequences that result from such a formulation.

1.5.4 The system of units describing small quantities

Volumes are associated with an exponent equal to 3, which is rather high. From the centimeter to the micrometer, volumes decrease by 12 orders of magnitude. In this context, it is useful to know some expressions used in the world of microsystems for describing extremely small quantities. We thus have the following table:

Name	Power
milli	10^{-3}
micro	10^{-6}
nano	10^{-9}
pico	10^{-12}
femto	10^{-15}
atto	10^{-18}
zepto	10^{-21}
yocto	10^{-24}

These small units are frequently used, a few examples of which are presented below. Volumes contained in microfluidic systems commonly range from about 10 to a few hundred nanoliters. A biological cell as we saw above is typically a sphere 10 μm in diameter, enclosing a volume of 4 pL. Reference [24] reaches a detection threshold of 15 amole (i.e. 15 atto-mole) by coupling a microfluidic system to a mass spectrometer. A recent study [25] showed that it is possible to detect the presence of a zeptomole of DNA by means of a miniaturized electrochemical method. The expressions 'atto' and 'zepto' are actually frequently used in the field of microsystems.

1.5.5 A few consequences of scaling laws in nature

We examine a few consequences of scaling laws in nature for plants and animals, scaling laws whose importance has already been presented by Galileo [26]. Scaling effects were discussed in detail more than a century ago by Sir D'Arcy Thomson, in a text [27] that even today remains an important reference. In the present day, these questions are still discussed: for example, the performances of giant extinct animals are still being investigated. What is the maximum velocity of the tyrannosaurus in the film 'Jurassic Park'? Did this animal run at 20 m/s, the speed of a jeep (as in the film), or did it only attain a speed of 11 m/s in its best moments (a result suggested by numerical simulation [21])? Here, we simplify the situations considerably, and only mention results that are both well accepted (at least along their main points) and also pertinent to orders of

magnitude. We take the example of small animals: they receive energy per unit time, coming from the food they eat, proportional to their weight (this pertains not only specifically to small animals, but to all animals). We thus have an input of chemical energy per unit time, which is equal to:

$$Q_N \sim l^3.$$

These animals transfer heat towards the outside, according to a law that can be established assuming that the transfer is made through a layer of thickness δ and surface area S. The amount of heat evacuated per unit time Q by the animal is thus:

$$Q = \frac{kS}{\delta}\Delta T,$$

where k is the conductivity of the surroundings and ΔT is the temperature difference between the body of the animal and the exterior. Considering that the surface S and the thickness δ vary as l^2 and l, respectively, we obtain the following scaling law for Q:

$$Q \sim l.$$

We also see that the smaller the organism, the more difficult it is to compensate for thermal losses by eating food, and thus the more difficult it is to maintain its internal temperature at a level substantially different from the exterior temperature[13]. We can see that for animals, there exists a lower limit to size beyond which thermal equilibrium cannot be assured. This limit is represented by the pygmy shrew, whose size is of a few centimeters (Fig. 1.15). Like some mythological victim of torture, this animal must permanently eat to maintain its internal temperature at a fixed level in order to survive. These scaling effects on thermal fluxes also explain why small insects can only survive by being cold-blooded (they are 'poïkilotherms'), at a non-imposed temperature.

Another example: at small scales, capillary forces dominate gravitational forces. This is what is indicated in Table 1.1. In effect, after taking the relevant exponents into account, it is easy to see that capillary forces clearly dominate gravitational forces in systems of small size. Capillary forces are associated with an exponent equal to 1, while gravitational forces are associated with an exponent equal to +3. One important consequence of the predominance of capillary effects on weight is that it is possible to walk on water thanks to wetting forces. In the case of walking on water, the foot of the insect is subjected to hydrophobic

[13] On the other hand, large animals have a difficult time getting rid of their thermal energy. The whale uses its blood circulation to transfer heat towards the exterior. When hunters killed a whale, its circulation stopped, the exchange of heat ceased, causing the internal tissues to cook. Hunters valued the meat of the whale cooked in this way.

Figure 1.15 This figure shows an ordinary shrew, which is 9 cm long and weighs a few grams. This animal ingests its own weight in insects, worms, and spiders on a daily basis. The pygmy shrew is even smaller, and must ingest food even more quickly to survive. The predator of the shrew is the weasel, who, because of its size, has more leisure time before meals. © Laurent Thouzeau/Bios.

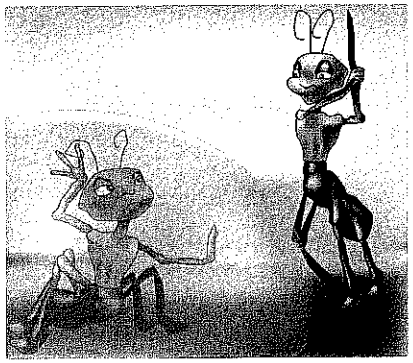

Figure 1.16 This drawing, inspired by a famous animated drawing, represents the significant effort it would take for an ant to free a comrade imprisoned in a bubble. At the scale of an ant, capillary forces are very significant with respect to the muscular forces the animal can exert. After [11].

forces maintaining it partially out of water. The effect of gravity, which tends to immerse the foot, is easily compensated for. In the same vein, we can see that it is not difficult for insects to climb up walls.

As emphasized by Kim [11], if we lived in a submillimetric world, the principal phenomenon that would concern us would be capillarity and not gravity or inertia. We would fear getting stuck to the surface of liquids, but we would not risk being hurt by an impact. At this scale, we would undoubtedly have invented (if our intelligence was still intact) numerous machines driven by surface tension. It would seem natural that in our microworld, automobile accidents would not be caused by collisions, but by drops of water abandoned in the road.

Capillary forces dominate gravitational forces at this scale, and even more easily dominate centrifugal forces (see Table 1.1). The scaling law for centrifugal forces is obtained by the following logic: we consider an object of size l and

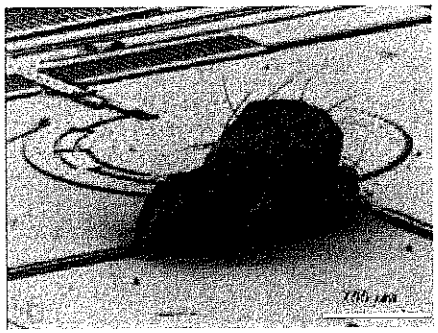

Figure 1.17 A mite from New Mexico placed on a micromotor (see the site of Sandia National Laboratories www.sandia.com). The film on the site shows the rotating motor does not eject the mite from the rotor, despite high rotation velocities. The mite's impressive performance can be explained by the scaling laws we are discussing here.

density ρ, placed on a micromotor rotating at a velocity of Ω. In these conditions, the centrifugal force is:

$$F_c \sim \rho \Omega^2 l^4.$$

It is thus not difficult for an insect such as the one shown in Fig. 1.17 to use the adhesion forces proportional to l^2 to cling to the motor. To fabricate the micromotor, this scaling law will allow the development of considerable velocities of rotation without risk of breaking rotating pieces.

We now look into the question of jumping heights of animals. Usually if one considers that muscular force increases proportionally with the square of the size of the animal. The argument is the following: a force is a stress times an area, and the maximum stress the muscle can develop depends on its constituents not on its size. The muscular energy necessary to make a movement of amplitude l is thus proportional to l^3. This quantity must be compared with the potential energy of the jump E_p, which has a value:

$$E_p \sim mgH \sim l^3 H.$$

Comparing the two energies, the height of the jump H is deduced to be on the order of l^0. The height attained is thus independent of the size of the animal. We can thus conclude that, in terms of scaling laws, the flea jumps just as high as the elephant[14].

[14] In passing, we can note that as the muscular force is proportional to l^2, it follows that the ant can only break a water bubble with difficulty. The force that it must exert to counteract capillary forces is on the order of l.

We conclude with the running of animals and the tyrannosaurus problem. The expression for the velocity $v = l/\tau$ of an animal that runs by displacing its feet at an amplitude l over a period of time τ. We assume that the feet function at a frequency near the resonance frequency of the biomechanical system made up of the foot and the knee. We thus have $\tau \sim 1/l$, which implies $v \sim l^0$. Thus, animals all run at about the same speed. This law is verified by orders of magnitude: for a mouse, a man, an elephant and a tyrannosaurus, the maximum attainable speeds are all on the order of ten or so meters per second. The controversy over the speed of tyrannosaurus, and those of other large prehistoric animals, does not have a bearing on orders of magnitude. The controversy is over whether this animal can actually run as fast as a jeep, or if it cannot even surpass the speed of a man. Here, it is necessary to take into account the structure of the joints, the flux involved in supplying the muscles, etc., a subject that we will not deal with here. We thus show several examples illustrating how physical laws governing small insects are different from those governing the macrometric world due to the fact that the force equilibria are different. As a final point we note that scaling laws can also involve exponents that are not fractions: the surface area of exchange of certain important organs involved in metabolism such as the lungs and the intestines have a fractal structure.

1.5.6 Range of applications of scaling laws

We have reasoned here using exponents without discussing in detail the physical laws in play. This approach has the advantage of being simple and direct, but at times it leads to conclusions that cannot be applied to microsystems, since the range of scales is shifted with respect to their size. The purpose of this section is to highlight this issue. We consider the problem of mixing in microsystems, and more specifically, the question of knowing whether the agitation of fluids can result in the reduction of mixing time in a microfluidic system. According to Table 1.1, we would expect that in microsystems, diffusion phenomena are much faster than hydrodynamic transport phenomena. A typical hydrodynamic transport time is:

$$\tau_a \sim \frac{l}{U} \sim l^0,$$

where, as has been the case throughout this chapter, l is the characteristic scale, and U is a typical speed. The molecular diffusion time is expressed as:

$$\tau_d \sim \frac{l^2}{D} \sim l^2,$$

where D is the diffusion coefficient. For miniaturized systems, and if we work things out using only exponents, we expect to have $\tau_a \gg \tau_d$ because the exponent for the transport time is equal to zero, while the exponent associated with diffusion time is equal to two. Given that the effect of molecular diffusion is to mix, we could conclude that in microsystems it is useless to agitate the fluid in order to accelerate the mixing process. However, in practice, such a conclusion would be extreme once actual numerical values are considered. Examine the more complete expressions for the two preceding characteristic times. Their ratio is a dimensionless number, the Peclet number:

$$Pe = \frac{\tau_d}{\tau_a} = \frac{Ul}{D}.$$

To illustrate its significance, we consider the case of fluorescein mixed with water in a volume of 100 μm, flowing at a rate of 30 μm/s. In such a situation, the Peclet number is: $Pe \approx 10$. This elevated value suggests that diffusion phenomena are acting much more slowly than hydrodynamic transport phenomena, a result contrary to that suggested by only examining the exponents of the terms. For mixing, we can see that the conditions under which a reduction in scale is sensible are those given by $Pe < 1$; in the previous example, this would necessitate a reduction of the volume dimensions by an order of magnitude in order to satisfy this criteria. Thus, in several situations, it is important to rationalize using physical laws in their more detailed form to ensure that the effect of miniaturization is significant within the range of dimensions on the order of ten or a hundred micrometers, which are the scales normally used in microsystems.

1.6 Miniaturization of electrostatic systems

1.6.1 Dielectric breakdown is retarded in miniaturized systems

The phenomenon of sparks between two electrodes originates from the fact that, when subjected to an intense electric field, gas molecules situated between two electrodes are ionized, thus forming a plasma. Ionization is propagated little by little by a cascade phenomenon: in such a process, a large number of electrons are liberated, and an intense electric current can circulate between the two electrodes. This current is accompanied by a luminous emission that gives rise to the phenomenon of the electric arc. In air, under normal conditions, the breakdown electric field strength is on the order of 30 kV/cm, which is generally considered to be a reference value.

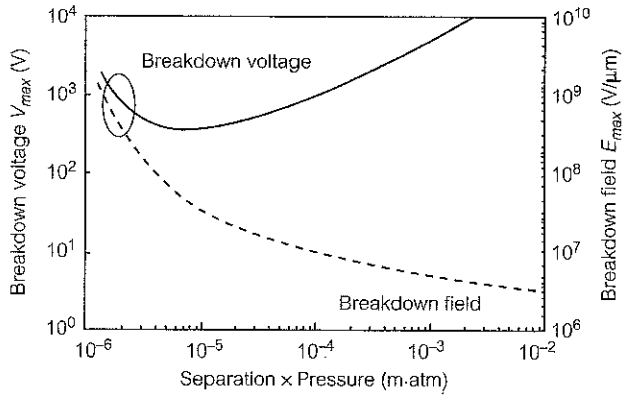

Figure 1.18 'Paschen curve': evolution of the potential difference and electric field strength of dielectric breakdown for a parallel-plate capacitor as a function of the product pressure × distance between electrodes; the curve is obtained in air.

In miniaturized systems, it is remarkable that much higher electric fields can be produced without the generation of an electric arc. This phenomenon is due to an effect of rarefaction that we will mention again in Chapter 2 under another form, pertaining to gas flows in microcanals. This effect is well represented by the Paschen curve, depicted in Fig. 1.18.

The Paschen curve represents the dielectric breakdown voltage between two electrodes, measured in air. This curve is shown along with the electric field, and is traced as a function of the pressure–distance product. We see that at large values of pressure × distance, the breakdown electric field strength E_d is:

$$E_d = 30 \text{ kV/cm}.$$

The curve shows that at small values of this product, the breakdown electric field strength increases significantly. This phenomenon is related to the fact that at small values of the pressure × distance product, the mean free path of the gas is on the order of the size of the system[15]. When the mean free path becomes comparable to the distance between electrodes, the majority of molecular collisions tend to take place between the gas and the surface, and not within the gas itself. This situation inhibits the formation of the cascade process and consequently makes it more difficult for an electric discharge to form in the gas.

[15] Under normal conditions in air, the mean free path is 61 nm. This value, much smaller than distances appearing on the figure, is nonetheless sufficiently high to induce a change of regime.

1.6.2 Miniaturization of capacitors

Many systems use miniaturized parallel-plate capacitors. We will consider this type of device as a prototype to establish the scaling laws involved in electrostatics. The electrostatic energy W_e stored by a parallel-plate capacitor is written:

$$W_e = \frac{1}{2}CV^2 = \frac{\epsilon_0 S V^2}{2d},$$

where C is the capacitance, S is the surface area of the plates, ϵ_0 is the dielectric constant, V is the voltage applied on the edges of the capacitor, and d the distance between plates. The forces used to displace one of the plates result in a gradient of this energy. For example, a displacement normal to the plane of the capacitor necessitates a force equal to:

$$F = -\frac{\delta W_e}{\delta z} = \frac{\epsilon_0 S V^2}{2d^2} \sim \epsilon_0 E^2 l^2$$

(z being an axis perpendicular to a plate), where E is the electric field created in the capacitor. In terms of scaling laws, and considering that the electric field strength is comparable to the breakdown field strength[16], we find that the energy varies as l^3, and the force as l^2. We have at our disposal an estimation of the *maximum* forces that can release an electrostatic system of a given size. This force could be compared to that which supplies, for example, the coupling of a current and a magnetic field. It seems in all cases that electrostatic forces are dominant over gravitational forces and inertia (which vary as l^3); there is thus no difficulty in exerting rapid accelerations in microsystems with the aid of electric fields. Such systems could promisingly be used as accelerometers (their weak inertia allows for the detection of sudden impacts, such as those involving automobiles).

1.6.3 An electrostatic microactuator

The possibility of creating elevated electric fields has led to the creation of a large number of electrostatic actuators. Figure 1.19 shows a simplified actuator, detailed in reference [28].

Here we have a beam and a base subjected to an electrostatic potential, thus forming the two plates of a capacitor. $f(x)$ is designated as the density of electrostatic attraction force (per unit surface) evaluated at the position x.

[16] Taking the preceding paragraph into account, it would be good to include a discussion on the phenomenon of the inhibition of electric breakdown in microsystems, though we do not introduce this aspect here.

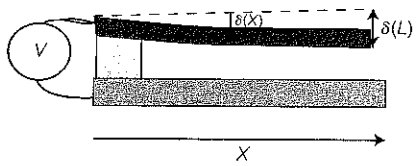

Figure 1.19. A cantilever beam, where the beam and the substrate are conductive. The beam is subjected to an electrical potential difference V, creating an actuator.

The expression of the density of force $f(x)$ can be obtained from the electrostatic force, given in section 1.6.2. We obtain:

$$f(x) = \frac{\epsilon_0}{2}\left(\frac{V}{d-\delta(x)}\right)^2,$$

where V is the applied voltage, ϵ_0 is the dielectric constant of the vacuum, d is the distance between the beam and the plate for $x = 0$, and $\delta(x)$ the deflection of the beam at the abscissa x (Fig. 1.19).

This force produces a deflection $\delta(x)$, which is controlled by a local elastic equilibrium, given by the relation:

$$\mathrm{d}\delta(x) = \frac{x^2}{6EI}(3L - x)wf(x)\mathrm{d}x$$

where E is the Young's modulus of the beam, I is its moment of inertia, L is its length and w is its width. We recall the expression of the moment of inertia of a beam of width w and thickness h:

$$I = \frac{1}{12}wh^3.$$

To determine the deflection at the end of the beam, one must integrate this equation. The profile of the beam is governed by the equation:

$$\delta(x) \approx \left(\frac{x}{L}\right)\delta(L).$$

This permits the determination of the relation between the total force F applied on the beam, and its relative maximum deflection given by:

$$\Delta = \delta(L)/d.$$

The calculation gives, in the limit of small deflections:

$$F = \frac{\epsilon_0 w L^4 V^2}{2EId^3} \approx \frac{4\Delta}{3}.$$

In terms of scaling laws, we see that the relative deflection Δ is expressed as:

$$\Delta \sim \frac{V^2}{l^2},$$

which shows that it is possible to obtain significant displacements by miniaturizing while maintaining a fixed potential difference (assuming that the breakdown field is not surpassed). This possibility, illustrated in the case of an extremely simple electrostatic actuator, is actually used in a large number of MEMS.

1.6.4 The electrostatic micromotor

The electrostatic micromotor is an example of a sophisticated and remarkable electrostatic actuator. An electrostatic micromotor made using MEMS technology is represented in Fig. 1.20a, and a diagram of its operating principle is shown in Fig. 1.20b.

The force produced by such a motor is:

$$F = -\frac{V^2}{2R}\frac{\partial C}{\partial \theta},$$

where R is the radius of the rotor, V is the applied voltage, C is the capacitance of the rotor/stator and θ is the angular variable. The arrows in Fig. 1.20 indicate that the stator produced a rotating field. The shaded areas of the rotor represent an inhomogeneity of the dielectric constant of the materials making up the rotor. The principle of how this motor functions lies in the fact that the rotor will try to align the region with the strongest dielectric constant with the regions with the strongest electric field. Since the field is rotating, the rotor will tend to follow the maxima of the field, and will thus begin to turn. To analyse the functioning of the motor, the forces in play must be averaged along the angular coordinate, taking into account the fact that the electrostatic field produced by

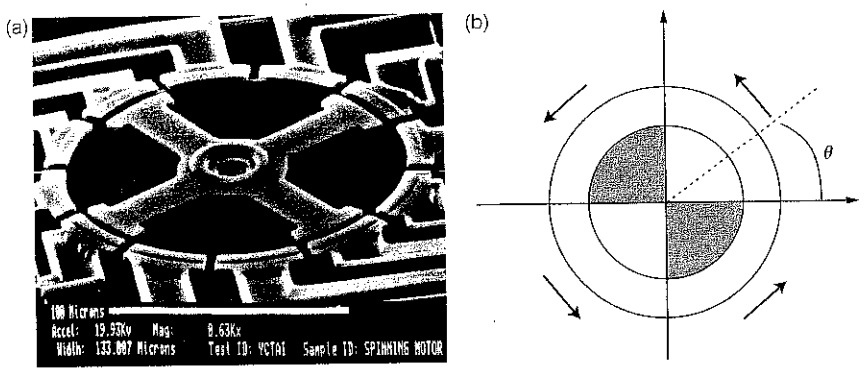

Figure 1.20 (a) First micromotor created in 1988 by Fan *et al.* [29]. The rotor has a diameter of 200 μm. (b) Diagram of the operating principle of an electrostatic motor. (photo courtesy of Richard S. Muller)

the stator is a rotating field. We will not perform this analysis, which is necessary for a more detailed comprehension of the system; we will instead reduce the calculation considerably by using scaling laws[17]. Using these scaling laws, the force is proportional to l^2, while the couple supplied by such a motor is proportional to l^3. Practically speaking, couples are produced on the order of nano- or piconewtonmeters, powers on the order of the microwatt, for thousands or tens of thousands turns per minute. Generally speaking, it is advantageous to envisage rapid rotations in order to produce significant power. Impressive devices are currently being created, including ones that function at several million turns per minute. One example is the turbine recently developed at MIT [30]. The objective here is to fabricate a millimetric microturbine that functions at 2.4 million turns/minute and produces 20 W with a yield of a few tens of per cent. A turbine like this, when put into rotation by combustion gases, would allow the conversion of chemical energy into mechanical and electric energy. We return here to the theme of miniaturization of energy sources, an extremely important subject in the field of MEMS.

1.7 Miniaturization of electromagnetic systems

We consider two conducting loops separated by a distance l, through which a current I passes (see Fig. 1.21).

Here, we assume that the cross-section of the wire carrying the electric current has a size comparable by order of magnitude to the diameter of the microcoil producing the magnetic field. This hypothesis can seem astonishing for a system of macrometric size: normally, the electromagnetic coils have cross-sections of

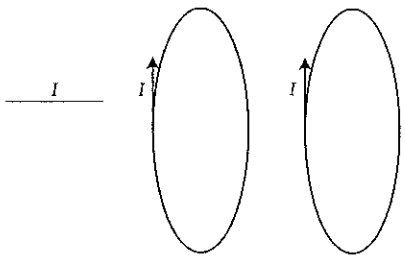

Figure 1.21 Diagram representing two conducting loops of characteristic size l, through which a current I passes, separated by a distance $O(l)$, i.e. a length on the order of l.

[17] This constitutes both the strength and the weakness of rationales based only on using orders of magnitude.

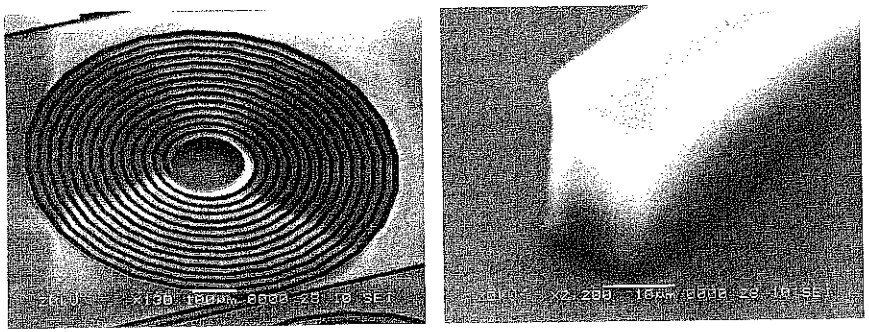

Figure 1.22 Microcoil created by the group of Fujita [31]. The figure on the right shows a conducting cross-section forming the microcoil.

wire that are much smaller than the diameter of the coil. This hypothesis is natural, however, for the microcoils created using microfabrication techniques presented in Chapter 6. An example is given in Fig. 1.22.

Thus, the magnetic field B produced by N turns is:

$$B \sim N\mu_0 jl$$

(this expression can be obtained in a variety of ways, for example by using Ampere's theorem). Here j is the current density, which we will consider to be fixed. We also deduce from this that the magnetic energy is:

$$E_{\mathrm{m}} \sim \frac{B^2}{\mu_0} l^3 \sim j^2 l^5.$$

These expressions show that it is difficult to produce elevated magnetic fields by miniaturizing standard electromagnetic elements, such as the coils. For a system with a size of 100 μm the maximum magnetic field that can be reasonably produced (without excessive heating) is on the order of 100 mT, which in a large number of situations would be considered to be a weak level of induction. This is a difficulty hampering the development of miniaturized electromagnetism for microsystems. For the forces between coils, we have:

$$F \sim jBl^3 \sim j^2 l^4.$$

We obtain the exponent from the scaling law table presented above. Consider also the case of a coil immersed in a fixed magnetic field, produced for example by a system of decimetric size. In this case, we determine the force applied on the coil using the law of Laplace

$$F \sim IBl \sim jBl^3,$$

where B is the magnetic field assumed to be constant. We see here that the force varies as l^3 if one performs the analysis at a fixed current density. In all cases, whether using a magnetic field produced locally or from the exterior, the exponents of the electromagnetic forces are higher than those associated with electrostatic forces[18].

To illustrate these calculations, we proceed to a comparison between electrostatic and electromagnetic microactuators. We recall the expression for electrostatic forces for a parallel-plate capacitor:

$$F \sim \epsilon_0 E^2 l^2,$$

where E is the breakdown electric field. For an electric field of 30 kV/cm and a device of 10 μm, we obtain:

$$F \sim 10 \text{ nN}.$$

For an electromagnetic system containing N coils in series, we have the following order of magnitude for the force:

$$F \sim \mu_0 N j^2 l^4.$$

Taking $N = 100$ coils, $j = 10^7$ A/m^2 and $l = 10$ μm, we obtain the following order of magnitude for the force exerted between two microcoils:

$$F \sim 100 \text{ pN}.$$

We verify, as would have been predicted using scaling law rationale, that the force produced by the microcoils is far less than that produced by a capacitor device. At which scale do electrostatic forces become dominant with respect to electromagnetic forces? We consider two 'prototypic' situations chosen arbitrarily: the case of the parallel-plate capacitor and that of mutually coupled coils. Re-examining the expressions established above, the scale that we find is on the order of a few hundred micrometers. More generally, we allow that ten or so micrometers correspond to the physical limit beyond which electrostatic forces begin to dominate over electromagnetic forces for optimized devices (which we have not considered here). Reference [28] presents a detailed discussion on this subject.

[18] We note that, in principle, it is possible to augment the current density in conductors, by maintaining (as we will see later) intense thermal exchanges in miniaturized systems. This possibility has not resulted in a definite answer, and the discussion is still open [28].

1.8 Miniaturization of mechanical systems

1.8.1 Microbeams resonate at elevated frequencies

A cantilever beam possesses a resonance frequency determined by the following relation:

$$f \approx \frac{hc}{2\pi L^2},$$

where h is the thickness of the beam, L is its length, and c is the speed of sound in the beam. This expression is obtained by resolving the elasticity equation. In terms of scaling laws, we have the relation $f \sim l^{-1}$. This law can be directly obtained by noting that an acoustic wave associated with the mechanical resonance has a wavelength on the order of the size of the object. We thus have the relation:

$$f \sim \frac{c}{l},$$

which corresponds to the expression deduced from the preceding formula.

The scaling law obtained here shows that the resonance frequency of a mechanical system increases as the size of the system diminishes. This characteristic is used to make resonators used in the domain of radiofrequency. Figure 1.23 shows an example of one particular setup for a miniaturized resonator, and Fig. 1.24 presents a recent creation obtained using MEMS technology [32].

In terms of orders of magnitude, we have for silicon:

$$c \approx 7470 \text{ m/s}.$$

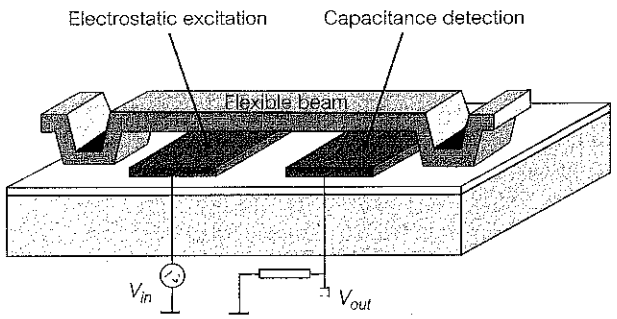

Figure 1.23 Diagram showing a mechanical resonator energized by an electric field. The material used for this mechanical resonator must be piezoelectric.

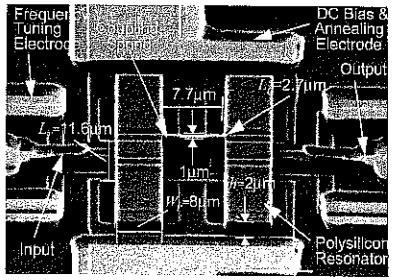

Figure 1.24 A resonator functioning at 75 MHz, made with silicon at the University of Michigan [32].

Thus, for a beam 1 μm thick and 3 μm long, the formula given above leads to

$$f \approx 100 \text{ MHz}.$$

Such a value is well suited for the field of radiofrequency.

We recall the definition of a quality factor, generally denoted as Q, for a system similar to a dampened oscillator. Such a system is governed by the following differential equation:

$$m\frac{d^2x}{dt^2} - b\frac{dx}{dt} - kx = 0,$$

where m is the mass of the spring, b is the attenuation coefficient, and k is the spring constant. For this type of system, the quality factor is:

$$Q = \omega_0 \frac{m}{b},$$

where ω_0 is the resonance frequency defined by:

$$\omega_0 = \sqrt{\frac{k}{m}}.$$

The quality factor characterizes the shape of the resonance curve. The form of such a curve is effectively given by the expression:

$$a(w) = \frac{1}{\sqrt{\left(1 - \frac{\omega^2}{\omega_0^2}\right)^2 - \frac{\omega^2}{Q^2\omega_0^2}}}.$$

The width of the resonance curve is thus directly related to the value Q: this width (calculated at mid-height, i.e. for a value of $a(\omega)$ equal to $\frac{1}{2}$), is in effect on the order of the inverse of Q. Thus, the higher the Q, the smaller the resonance. The factor that limits Q is, in this presentation, the friction represented by the coefficient b.

In the case of the vibrating beam, an equation analogous to the dampened oscillator can be established. In this case, the variable x is the maximum deflection of the beam, the damping factor b is proportional to the viscosity of the surrounding fluid, and the spring constant k is a function of the Young's modulus of the material and the geometrical characteristics of the beam.

For a cantilever beam, the quality factor (for regimes of non-rarefied gas) is estimated by the expression [28]:

$$Q = \frac{\sqrt{E\rho}wh^2}{24\nu L^2},$$

where ν is the kinematic viscosity of the gas and E is the Young's modulus of the material forming the beam. This law is not very favorable when the quality factor decreases with the scale. However, in practice, quality factors of ordinary microresonators can attain elevated values (on the order of 1000). The law obviously encourages operation in a vacuum, where the highest quality factors are obtained (between 10^4 and 10^5).

1.8.2 Thermal noise limits the quality factor of microresonators

It is instructive to calculate, for a cantilever beam, the displacement induced by thermal noise. This calculation provides a good example of a phenomenon of insignificant amplitude in systems of decimetric size; yet the importance of this phenomenon becomes considerable in miniaturized systems.

At thermodynamic equilibrium, elastic energy balances thermal (according to the equipartition theorem). We thus have:

$$\frac{1}{2}k < \delta^2 > = \frac{1}{2}k_B T,$$

where δ is the displacement of the beam, k is the constant recalling the mechanical system (that we again compare to a spring), k_B is the Boltzmann constant, and T is the temperature. We then show that this equation leads to the following expression for the 'thermal' displacement δ:

$$\delta \approx \sqrt{\frac{2k_B TL^3}{Ewh^3}},$$

where E is Young's modulus, L is the length, h is the thickness and w is the width of the beam. In terms of scaling laws, we thus have the following relation:

$$\delta \sim l^{-1/2}$$

which shows that the more we miniaturize, the larger the thermal displacement. From a numerical point of view, the thermal displacement for a silicon beam of 1 μm is on the order of a picometer. This is a very small displacement, but it is enough to limit achieving high quality factors for microresonators.

1.9 Miniaturization of thermal systems

Heat transfers by conduction are governed by the Fourier equation, which is written:

$$q = -K\nabla T,$$

where K is the thermal conductivity of the medium, T is the local temperature, and q is the heat flux, i.e. the quantity of heat traversing a surface element per unit surface (the units of q are thus energy per unit time and surface). The flux density varies as the inverse of the scale, at a fixed temperature difference. A typical situation is a bar thermally isolated on the sides, and whose ends are in contact with two thermostats that impose a temperature difference $\Delta T = T_2 - T_1$ (Fig. 1.25). Under these conditions, the heat flux going through such a bar is written:

$$Q = \frac{KS\Delta T}{l},$$

where S is the cross-sectional area of the bar, and l is its length. The following scaling law comes from this:

$$Q \sim Kl\Delta T,$$

which governs the heat flux. This law corresponds to the law shown in the general scaling law table, with the assumption that the temperature difference is fixed.

We now suppose that there exists in the bar sources of volumetric heat: we cite for example a Joule heating effect (if the bar is a conductor of electricity, and subjected to an electromagnetic field), or heating from a chemical origin (if the bar is the site of exothermic reactions). In both these cases, we can consider that the heat produced by a volumetric source is:

$$Q_v \sim l^3,$$

which represents an exponent much higher than that associated with heat evacuated by conduction. We can thus conclude that volumetric heat sources can be easily thermalized in miniaturized systems. One example of a microexchanger currently on the market is shown in Fig. 1.26.

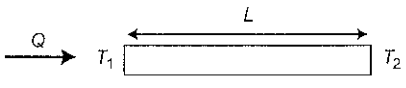

Figure 1.25 Diagram representing a bar carrying a heat flux Q, with notations used in the text.

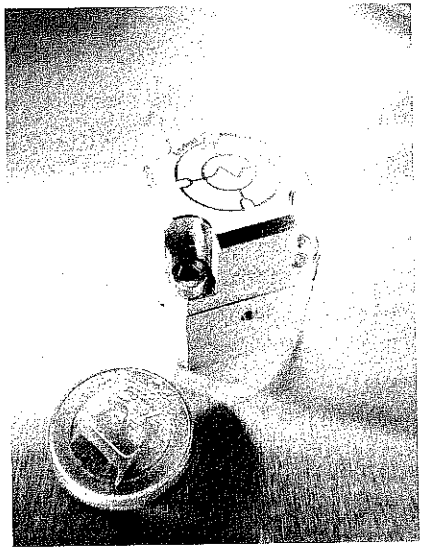

Figure 1.26 Microexchangers on chip, commercialized by the company Ehrfeld Microtechnik. Their size is comparable to a euro.

It is interesting to consider this from a dynamic point of view: the heat flux (stored or dissipated) associated with a temporal variation of temperature $\mathrm{d}T$ and a time $\mathrm{d}t$, is governed by the following relation:

$$q = \rho C_\mathrm{p} \frac{\mathrm{d}T}{\mathrm{d}t},$$

where ρ is the volumetric mass, C_p is the specific heat at constant pressure, and t is the time. Thus the order of magnitude of the time constant of thermalization associated with an object of dimension l is written:

$$\tau \sim \frac{\rho C_\mathrm{p}}{K} l^2 \sim \frac{l^2}{\kappa},$$

where κ is the thermal diffusivity of the environment under consideration. Consistent with the preceding remarks this expression shows that miniaturization considerably accelerates the return to thermal equilibrium of the bulk subjected to a sharp temperature change. In other words, miniaturization radically reduces the significance of the phenomena of thermal inertia. The preceding logic shows that exo- or endothermic chemical reactions can in principle be finely thermalized in microsystems. This characteristic is very useful for chemical engineering. In general, temperature exchangers currently used by industrial reactors tend to develop unwanted parasite reactions. These reactions limit the 'selectivity' of the

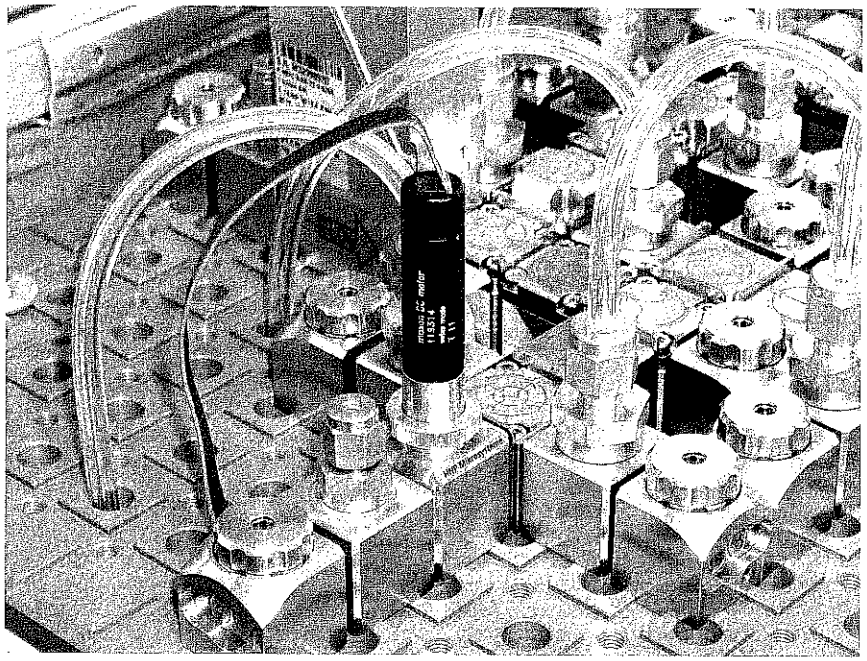

Figure 1.27 Microreactors commercialized by the company Ehrfeld Microtechnik. In the photo, they are assembled with other elements (microexchangers, microfilters, etc.) in such a way as to create a chemical microfactory. The side of an Ehrfeld cube has a measurement of about 2 cm. This system is more a matter of mini-space rather than microfluidics.

process. There are also reactions, impossible to use industrially, that can inherently control thermal conditions. For these types of systems, miniaturization offers a source of important improvements. Companies such as Ehrfeld have proposed the building of microreactors that can complete chemical engineering processes (Fig. 1.27).

1.10 Miniaturization of systems for chemical analysis

In the following chapters we will describe several physico-chemical transformations that take place in laboratories on chip. Here, we mention two physical problems in miniaturized systems of analysis that can present themselves during sampling, detection, and post-treatment.

1.10.1 Microdroplets evaporate rapidly

Microsystems are often closed systems, communicating with the exterior world indirectly via sensors and microfluidic connections. We can imagine inserting access to the outside world in different places in these systems. These could be, for example, a microcanal used to transport chemical reactants that is connected to chambers open to the exterior. When such a system is created, different problems arise. Evaporation of liquid is one of these problems. The evaporation of a drop of diameter d at time t is governed by the 'D^2 law' which reads:

$$d^2 = d_0^2 - \beta t$$

in which d_0 is the initial diameter, and β is independent of the drop size. The time τ it takes for the drop to disappear is thus:

$$\tau = \frac{d_0^2}{\beta} \sim l^2$$

Miniaturization thus favors rapid evaporation of droplets, and this phenomenon must be taken into account when droplets form in microsystems, whether or not they are destined for chemical use.

1.10.2 Is there even a molecule in the chamber?

One question poses itself for components present in weak concentrations in a given sample: is there a sufficient number of molecules to transfer into the analysis microchamber for detection? We calculate a few orders of magnitude: the volume containing an isolated molecule is given by:

$$v = \frac{1}{CN_A},$$

where C is the concentration of the chemical species in consideration and N_A is Avogadro's number. Thus, for a chamber with a side of 10 μm, the minimum concentration providing one molecule per analysis chamber is on the order of 10^{-12} mol/L. It is not certain that such a level is reached when the component to be analysed is presented in trace form. The problem is presented differently for DNA, because it is possible to use an amplification step (PCR) before analysis in a microsystem. For other molecules, amplification is not generally possible, and it is often necessary to apply a concentration step before detection. Here we come across many methods well known in the field of chromatography.

References

[1] J. Israelachvili, *Intermolecular and Surfaces Forces*, Academic Press, 2nd edn, 1991.

[2] J. Israelachvili, *Chemtracts-Anal Phy. Chem.*, 1, 1 (1989).

[3] D. Tabor, *J. Colloid Interf. Sci*, 58, 2 (1977).

[4] C. Tabor, R. Winterton, *Proc. R. Soc. Lond. A*, 312, 435 (1969).

[5] E.M. Lifschitz, *Soviet Phys. JETP (Eng. Transl.)*, 2, 73 (1956).

[6] B. Cabane and S. Hénon, *Liquides. Solutions, Dispersions, Émulsions, Gels*, Belin, 2003.

[7] H. Taunton, C. Toprakciaglu, L. Fetters, J. Klein, *Macromolecules*, 23, 571 (1990).

[8] Jacobson, Alarie, Ramsey, *Proc. μTAS*, 608 (2002).

[9] G. Karniadakis, A. Beskok, *Micro Flows*, Springer Verlag, 2002.

[10] In the 1990s, S. Chu made the first observations of the conformation of strands of elongated DNA at the intersection of two microcanals. One more recent reference is Smith, D., Chu, S., *Science*, 281, 1335 (1998).

[11] C.J. Kim, *Proc. Symp. Micromachining and Microfabrication*, 4177, Sant-Khandurina, R. Foote, J. Ramsey, *Anal. Chem.*, 70, 158 (1998).

[12] N. Crisona, T. Strick, D. Bensimon, V. Croquette, N. Cozarelli, *Gene Dev.*, 14, 22, 2881 (2000).

[13] C. Li, D. Harrison, *Anal. Chem.*, 69, 1564 (1997).

[14] F. Morin, M. Denoual, L. Griscom, B. LePioufle, J. Fujita, E. Tamiya, *Proc. μTAS*, 515 (2002).

[15] P. Renaud, U. Seger, S. Gawad, *Proc. Nanotech 2002*, Montreux (2002).

[16] D. Smith, H. Babcock, S. Chu, *Science*, 283, 1724 (1999).

[17] S. Lee, Y. Tai, *Sens. Actuators*, 73, 74 (1999).

[18] T. Lehnert, R. Netzer, U. Bischoff, M. Gijs, *Proc. Nanotech 2002*, Montreux (2002).

[19] A.Y. Fu, H.P. Chou, C. Spence, G.H. Arnold, S.R. Quake, *Anal. Chem.*, 74, 2451, (2002).

[20] E. Altendorf, Zebert, M. Holl, A. Vannelli, C. Wu, C. Schulte, *Proc. μTAS*, 73 (1998).

[21] J.R. Hutchinson, M. Garcia, *Lett. Nature*, 415, 1018 (2002).

[22] A.Y. Fu, C. Spence, G.H. Arnold, S.R. Quake, *Nature Biotechnol.*, 17, 1109 (1999).

[23] E. Guyon, J.P. Hulin, L. Petit, *Hydrodynamique Physique*, CNRS Edition, 2nd edn, 2001.

[24] Q. Wang, A. Desai, Y. Tai, L. Licklider, T. Lee, *Proc. MEMS* Orlando, 523 (1999).

[25] T. Wang, S. Masset, C.M. Ho, *Proc. MEMS 2001*, Interlaken, 431 (2001).

[26] Galileo Galilei, *Dialogue Concerning Two New Sciences*, 1638.

[27] D'Arcy Thompson, *On Growth and Form*, revised version, Camb. Univ. Press (1942).

[28] G. Kovacs, *Micromachined Transducers*, WCB, McGraw Hill, 1998.

[29] L.C. Fan, Y.C. Tai, R.S. Muller, *IEEE Trans. Electron. Devices*, ED-35, 6, 724 (1988).

[30] C.M. Spadaccini, X. Zhang, C.P. Cadou, N. Miki, I.A. Waitz, *Proc. MEMS 2002*, 228–232 (2002).

[31] L. Houlet, G. Reyne, T. Iizuka, T. Bourarina, E. Dufour-Gergam, H. Fujita, SPIE International Symposium on Microelectronics and Micro-Electromechanical Systems, Adelaide (Australia), 4592, 17–19, December 2001.

[32] A-C. Wang, J.R. Clark, C.T.-C. Nguyen, *Digest of Technical Papers*, 10th International Conference on Solid-State Sensors and Actuators, Sendai (Japan), June 1999.